SUPPLEMENTARY FIGURES

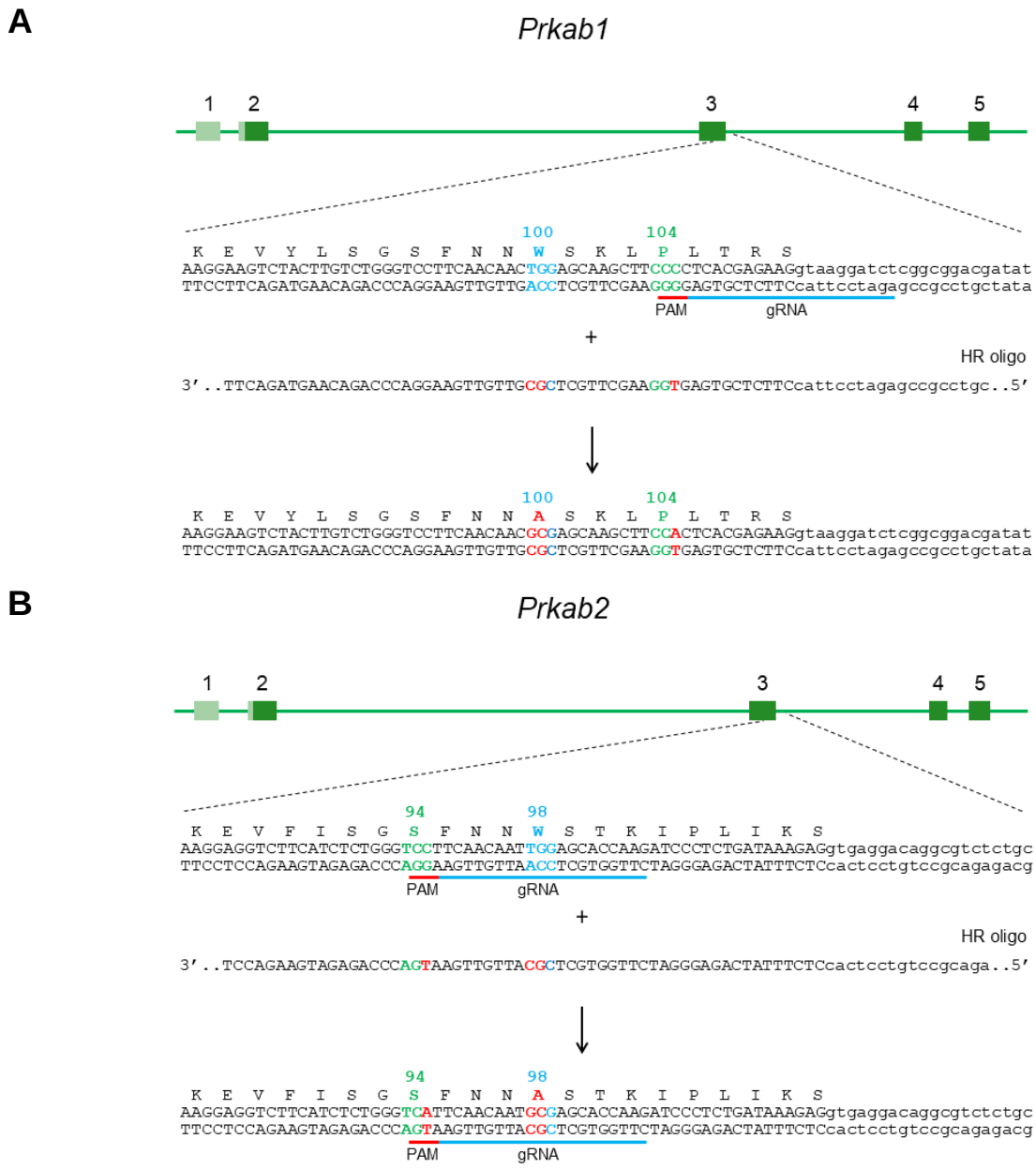

Supplementary Figure S1. Related to Figure 1. Gene targeting strategy used to generate AMPK β1 W100A and β2 W98A whole-body KI mice.
Prkab1^{W100A} (β1 W100A KI) and *Prkab2*^{W98A} (β2 W98A KI) mice were produced using CRISPR/Cas9 gene targeting in C57BL/6J mouse embryos following established molecular and animal husbandry techniques. Single guide RNAs (sgRNA) were based on target sites in exon 3 of *Prkab1* (AGATCCTTACCTTCTCGTGA*GGG*) and *Prkab2* (CTTGGTGCTCCAATTGTTGA*AGG*) (protospacer-associated motif [PAM] italicized and underlined). (**A**) For *Prkab1*, the oligonucleotide encoded the W100A (TGG>GCG) substitution plus a PAM-inactivating silent mutation in the P104 codon (CCC>CCA), while (**B**) for *Prkab2*, the oligonucleotide encoded the W98A (TGG>GCG) substitution plus a PAM-inactivating silent mutation in the S94 codon (TCC>TCA).

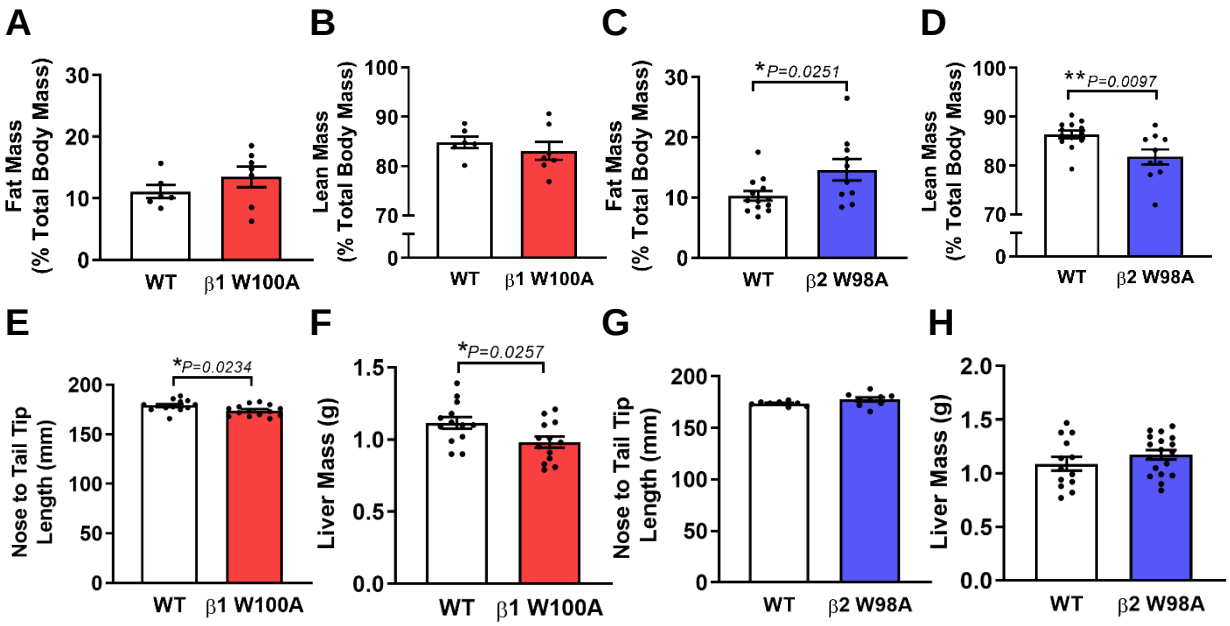

Supplementary Figure S2. Related to Figure 2. Disrupting AMPK β2 glycogen binding increases whole-body adiposity.

Male age-matched mice (8-15 wk) were subjected to EchoMRI analyses. (**A**) Fat and (**B**) lean mass for WT and β1 W100A (n=6-7), or β2 W98A (**C**) fat and (**D**) lean mass (n=10-13) are shown relative to total body mass. (**E**) Nose to tail tip length and (**F**) absolute liver mass for WT and β1 W100A (n=13-14; 14-22 wk), and WT and β2 W98A (**G**) nose to tail tip length and (**H**) absolute liver mass (n=8-18; 17-26 wk) are shown. Data are represented as mean ± SEM; **P* < 0.05; ***P* < 0.01.

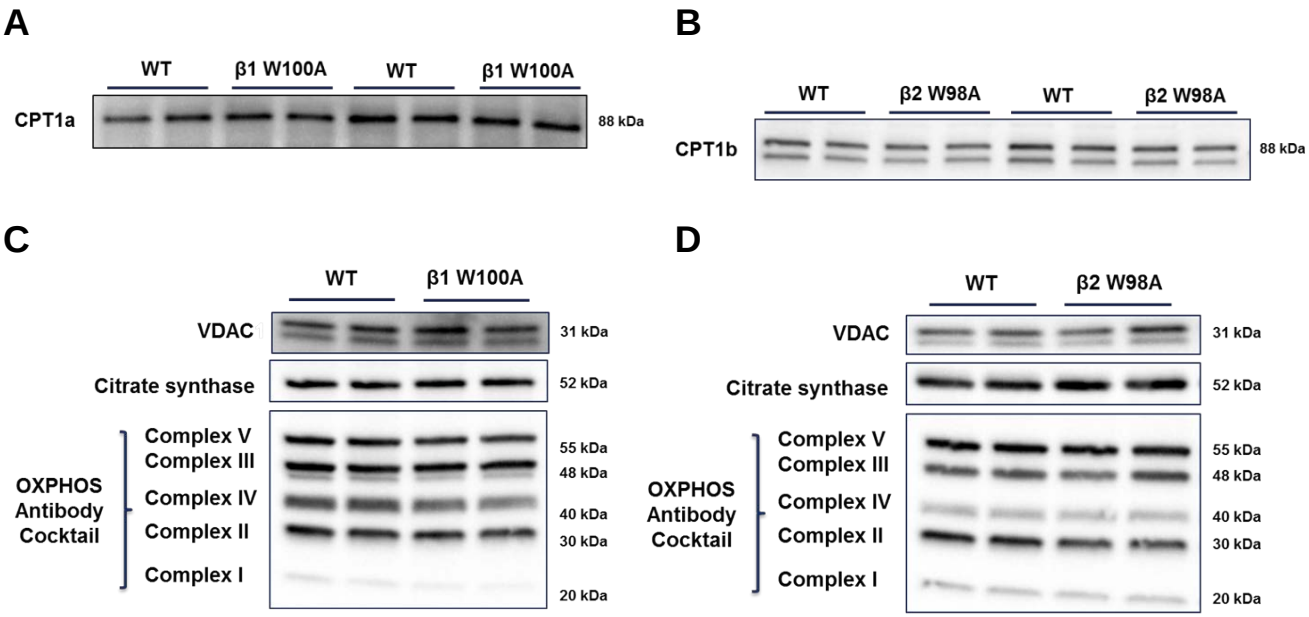

Supplementary Figure S3. Related to Figure 3. Liver and skeletal muscle fatty acid transporter and mitochondrial content are not different between β1 W100A, β2 W98A and respective WT mice. Tissues were collected from male age-matched WT and KI mice (ranging from 14-32 wk). Representative immunoblots processed in parallel are shown for fatty acid transporters (**A**) CPT1a in WT and β1 W100A liver and (**B**) CPT1b in WT and β2 W98A gastrocnemius muscle. Representative immunoblots processed in parallel are shown for mitochondrial markers VDAC, citrate synthase and OXPHOS complexes (Complex I, II, III, IV and V) in respective WT and (**C**) β1 W100A liver or (**D**) β2 W98A gastrocnemius muscle. Equal protein loading was confirmed using Bio-Rad stain-free imaging technology.

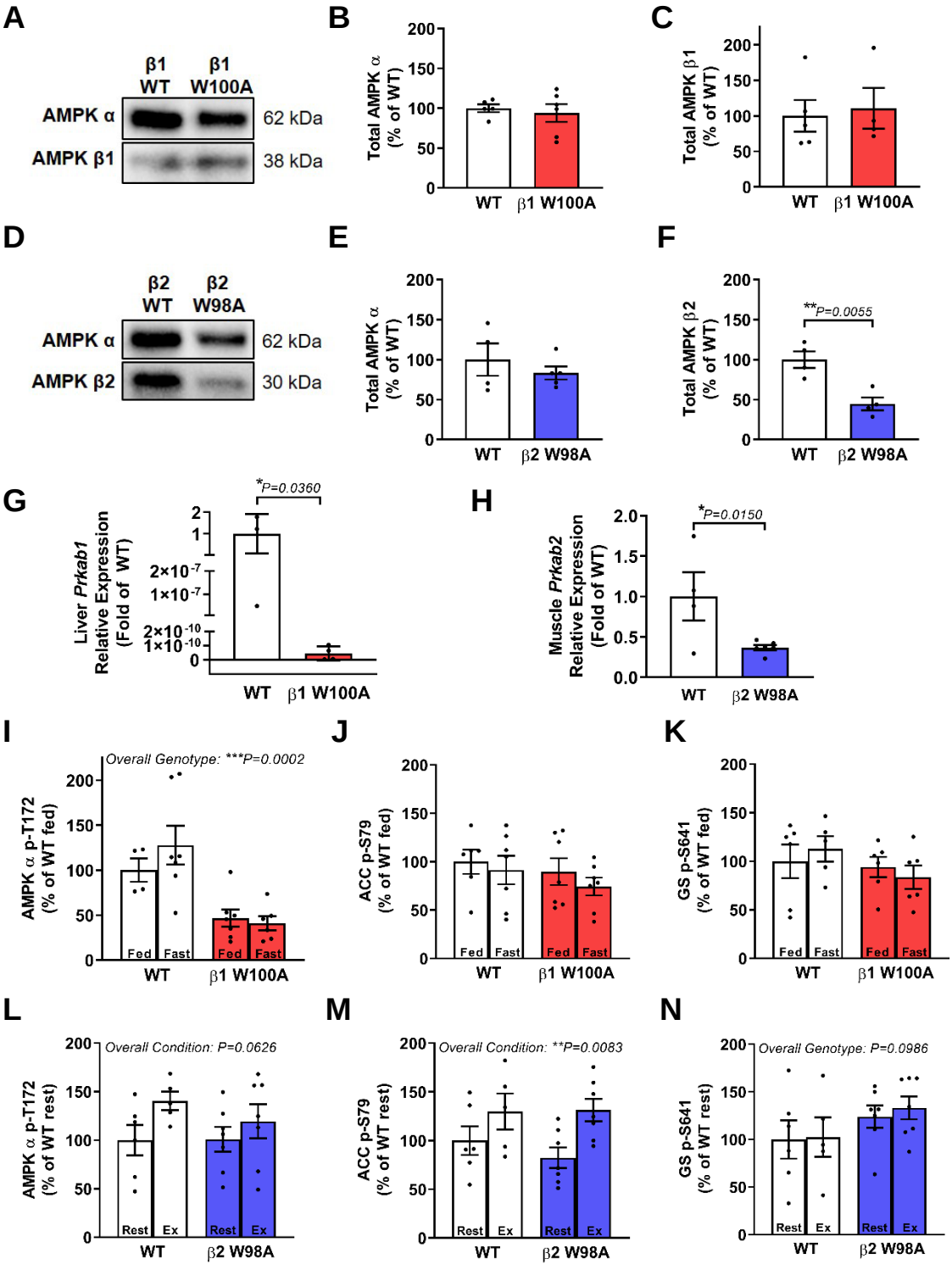

Supplementary Figure S4. Related to Figure 4. Disrupting AMPK β2 glycogen binding decreases adipose tissue AMPK β2 protein, and AMPK β1 W100A liver and β2 W98A muscle display respective decreases in *Prkab1* and *Prkab2* gene expression versus WT.

Tissues were collected from male age-matched WT and KI mice (ranging from 12-22 wk). Representative immunoblots processed in parallel are shown for respective WT versus (**A**) β1 W100A adipose tissue or (**D**) β2 W98A adipose tissue. Equal protein loading was confirmed using Bio-Rad stain-free imaging technology. Quantified immunoblots of adipose tissue total AMPK (**B**) α and (**C**) β content from WT and β1 W100A mice (n=4-6), and adipose tissue total AMPK (**E**) α and (**F**) β content from WT and β2 W98A mice (n=4-5) are shown. Relative *Prkab1* (AMPK β1) gene expression (**G**) in WT and β1 W100A liver (n=3-4) and relative *Prkab2* (AMPK β2) gene expression (**H**) in WT and β2 W98A gastrocnemius muscle (n=4-6) are shown. Quantified ratios of phosphorylated (**I**) AMPK T172, (**J**) ACC S79 and (**K**) GS S641 from fed and fasted WT and β1 W100A liver (n=4-7), and phosphorylated (**L**) AMPK T172, (**M**) ACC S79 and (**N**) GS S641 from WT and β2 W98A gastrocnemius muscle (n=5-7) are shown. Data are represented as mean ± SEM; **P* < 0.05; ***P* < 0.01.